

Małgorzata KMIOTEK ¹, Robert SMUSZ ²

Effect of thin obstacles heights on heat transfer and flow characteristics in microchannels

Received 6 September 2023, Revised 5 November 2023, Accepted 5 December 2023, Published online 23 December 2023

Keywords: micro-, computational fluid dynamics, microchannel, heat transfer

This paper presents a numerical analysis of the thermal-flow characteristics for a laminar flow inside a rectangular microchannel. The flow of water through channels with thin obstacles mounted on opposite walls was analyzed. The studies were conducted with a low Reynolds number (from 20 to 200). Different heights of rectangular obstacles were analyzed to see if geometrical factors influence fluid flow and heat exchange in the microchannel. Despite of the fact that the use of thin obstacles in the microchannels leads to an increase in the pressure drop, the increase in the height of the obstacles favors a significant intensification of heat exchange with the maximum thermal gain factor of 1.9 for the obstacle height coefficient $h/H = 0.5$, which could be acceptable for practical application.

Nomenclature

f	friction factor, –
H	height of the microchannel, m
h	height of the obstacle, m
h_x	heat transfer coefficient, $W/m^2 \cdot K$
k	thermal conductivity, $W/m \cdot K$
L	length of the microchannel, m
Nu	Nusselt number, –
T	temperature, K
T_{in}	inlet temperature, K
T_f	fluid temperature, K

✉ Małgorzata KMIOTEK, e-mail: kmimal@prz.edu.pl

¹Rzeszow University of Technology, The Faculty of Mechanical Engineering and Aeronautics, Department of Aircraft and Aircraft Engines, Rzeszów, Poland; ORCID: 0000-0003-3229-0367

²Rzeszow University of Technology, The Faculty of Mechanical Engineering and Aeronautics, Department of Thermodynamics, Rzeszów, Poland; ORCID: 0000-0001-7369-1162



T_w	wall temperature, K
p	pressure, Pa
Re	Reynolds number, –
s	spacing, m
U, V	dimensionless components of velocity
u, v	components of velocity, m/s
u_{in}	inlet velocity, m/s
w	width of the obstacle, m
X, Y, Z	dimensionless coordinates
x, y, z	Cartesian coordinates, m/s

Greek symbols

μ	dynamic viscosity, Pa·s
ρ	density, kg/m ³
η	thermal enhancement factor, –

1. Introduction

The miniaturization of electronic devices in which heat is generated makes it necessary to design efficient and miniaturized cooling systems. One of such solutions is the application of microchannels, which are now often used to cool electronic devices. However, due to the laminar flow of the cooling medium, the intensity of heat transfer is low. Hence, there is a need for intensification of heat transfer, for example by application of turbulising inserts, porous material, or internally ribbed walls, obstacles, etc. Usually the height of microchannel is the smallest linear dimension therefore channels with the smallest linear dimension which is less than 1 mm and greater than 1 μm are called microchannels. The use of obstacles on the walls of channels causes increased heat and mass transfer, which has been confirmed and presented in the literature [1–6]. In these studies of heat transfer in channels, the influence of the following parameters on the intensification of heat transfer was analyzed: Reynolds number, Nusselt number, Prandtl number, channel height H , obstacle height h , its width w and spacing s .

For example, in the work [7], the authors experimentally and numerically studied the turbulent flow in a channel with two baffles. Obstacles for which $h/H = 0.55$ (see Fig. 1), $w/h = 0.125$ (w – obstacle thickness) were installed on opposite walls of the channel at a distance of $s = 0.98H$. The authors found that large differences in pressure and velocity distribution occur where a high pressure area forms along both obstacles and a low pressure area forms across the obstacles due to the existence of vortex zones behind the obstacles. In [8], the authors presented the analysis of thermal flow in a channel with a height of $H = 40$ mm and with a series of thin solid and porous obstacles of constant width $w = 1.5$ mm placed on the walls of the channel at a constant distance of $s = 1H$. Obstacles of different heights ($h/H = 0.25; 0.5; 0.75$) were tested. It was shown that there was an increase in the value of Nusselt number for both types of

obstacles in relation to the smooth channel. As in the case of macrochannels, in order to intensify heat exchange in microchannels, obstacles should be placed [9–17]. To move the concept of obstacles from macrochannels to microchannels, it is necessary to know how strongly the geometrical parameters of obstacles influence the flow and heat transfer in the micro scale. The study results can be applied in various fields of micro devices. Some of the examples are micro heat exchangers or micro-mechanical systems [18]. The flow in such micro heat exchangers is laminar, so we should describe the flow to get higher rate of heat exchange.

The literature review of hydrodynamic parameters in microchannels with obstacles placed on walls shows that the emplacement of obstacles in microchannels' fluid flow creates additional recirculation zone, which affects mass and heat transfer, which in turn determine the efficiency of micro flow systems [19, 20]. Most of the published studies show thermal-flow characteristics in microchannels with obstacles placed on the walls, where the parameters of obstacles have an aspect ratio $w/h \geq 1$. There are only a few papers dedicated to investigation of fluid flow through microchannels with thin obstacles, which have aspect ratio $w/h < 0.5$. The application of thin obstacles located in the microchannels is desired for saving material.

For example, in [21] the authors analyzed and considered the influence of different geometries of the thin obstacles. The influence of one thin obstacle of triangular and rectangular shape on fluid flow in 2D microchannels, for very low Reynolds numbers was considered. The results showed that flow in the recirculation zones, behind the obstacles, is highly influenced by the geometrical parameters of the obstacle. Additionally, the obstacle of the rectangular shape provokes larger vortex formation in the recirculation zone. In turn, the two-dimensional stationary heat and fluid flow in a microchannel with two obstacles was presented in papers [22, 23]. In the microchannel with a height of H , obstacles were placed on the lower and upper wall at different distances (from $1H$ to $5H$). In the channel, two obstacles of relative heights $h/H = 0.33; 0.66$ were placed one after the other. The research was performed for Reynolds number range: $Re = 5; Re = 20, Re = 50$. The results showed that parameters such as height, distance between obstacles, and Reynolds number strongly influence the length of the recirculation zones behind the obstacles. The increase in length of the recirculation zone behind the obstacle and the increase in the Nusselt number are related to the increase of Re and height of the obstacles. Authors in [24] presented results of numerical and experimental analysis of fluid flow for the 3-baffled microchannels. The effect of obstacle height and Reynolds number on fluid mixing was investigated. The thin baffles with different heights $h/H = 0.625, 0.75, 0.875$ were investigated. The results showed that the increased fluid mixing was affected by the baffle height and Reynolds number. The increase in baffle height and Reynolds number produces a buildup of the recirculation zone, increase of convective mixing and stronger pressure drop.

In this paper, two-dimensional fluid flow in a microchannel with four thin obstacles has been investigated. We focus on the influence of height of the thin

obstacles spaced by a distance $s = H$ and on the influence of change of the Reynolds number on the creation of the recirculation zones and heat transfer characteristics. The height of the obstacle is shown to cause significant changes in the flow field, heat transfer and the friction factor compared to the smooth microchannel. The study of influence of obstacles' height change on fluid flow and heat transfer is carried out to determine transport effects and to receive practical results.

2. Problem formulation

The governing equations written in Cartesian coordinates are given by continuity equation, momentum equation and energy equation as follows:

$$\frac{\partial u}{\partial x} + \frac{\partial v}{\partial y} = 0, \quad (1)$$

$$\rho \left(u \frac{\partial u}{\partial x} + v \frac{\partial v}{\partial y} \right) = -\frac{\partial p}{\partial x} + \mu \left(\frac{\partial^2 u}{\partial x^2} + \frac{\partial^2 v}{\partial y^2} \right), \quad (2)$$

$$\rho \left(u \frac{\partial u}{\partial x} + v \frac{\partial v}{\partial y} \right) = -\frac{\partial p}{\partial y} + \mu \left(\frac{\partial^2 u}{\partial x^2} + \frac{\partial^2 v}{\partial y^2} \right), \quad (3)$$

$$\rho \left(u \frac{\partial T}{\partial x} + v \frac{\partial T}{\partial y} \right) = k \left(\frac{\partial^2 T}{\partial x^2} + \frac{\partial^2 T}{\partial y^2} \right), \quad (4)$$

where u, v are components of the velocity vector $V = (u, v)$, ρ, p, μ are the fluid density, the fluid pressure, the fluid dynamic viscosity coefficient, respectively, T, k are temperature, the thermal conductivity coefficient, respectively. It was assumed, that the fluid was incompressible, the flow was two-dimensional and laminar. Temperature and velocity were fixed at the inlet to the channel.

In this work, the issue of fluid flow and the process of convective heat exchange in a microchannel with obstacles of various heights and constant spacing were investigated. The geometry of the microchannel with obstacles is shown in Fig. 1.

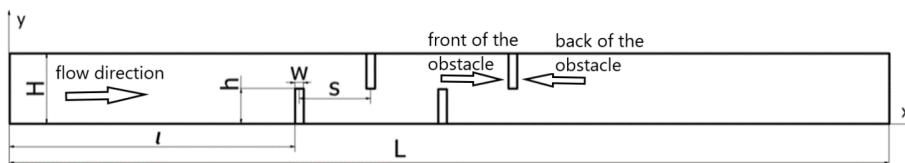


Fig. 1. Computational domain

The issue was defined as follows: in a microchannel of length L and height H , the first obstacle is placed at a distance l from the inlet to the channel (see Fig. 1). All obstacles were rectangular in shape (width w and height h) and were placed at the bottom and top of the channel walls. In addition, the distance between adjacent obstacles was s . The constant temperature and velocity were applied at

the channel inlet. The stream rise gradients of the velocity components at the outlet are assumed to be zero.

The boundary conditions are described as follows:

- 1) at the microchannel inlet: $x = 0, 0 \leq y \leq H, u = V, v = 0, T = T_{in}$;
- 2) at the microchannel outflow: $x = L, 0 \leq y \leq H$;
- 3) at the wall of the microchannel (non-slip velocity conditions and temperature conditions), i.e., $y = 0, u = v = 0; y = H, u = v = 0, T = T_w$;
- 4) at the obstacle wall of the microchannel (non-slip velocity conditions and temperature conditions), i.e., $u = 0, v = 0, T = T_w$.

The microchannel geometry was as follows: length (L) and height (H) were $5 \cdot 10^{-3}$ m and $400 \cdot 10^{-6}$ m, respectively. The obstacles were characterized by variable height (h) and constant width (w) of $50 \cdot 10^{-6}$ m, spacing (s) of $s = 1H$. The obstacles were on the top and bottom wall of the channel. The first obstacle was placed at a distance (l) of $2 \cdot 10^{-3}$ m from the beginning of the channel. The working fluid is water. The physical properties of water used in calculations are: $\rho = 998.3 \text{ kg/m}^3, \mu = 0.001 \text{ Pa}\cdot\text{s}$.

To investigate the thermal-flow performance of the microchannel, the following definitions of the parameters were applied.

Fluid flow was characterized by the Reynolds number, which was defined as:

$$\text{Re} = \frac{\rho V H}{\mu}, \quad (5)$$

where ρ denotes the density of the fluid, V denotes inlet fluid velocity, H is height of the microchannel and μ is the dynamic viscosity coefficient of the fluid.

Heat transfer was characterized by the local Nusselt number, which was defined as:

$$\text{Nu}(x) = \frac{h_x H}{k}, \quad (6)$$

where h_x, k are the heat transfer coefficient, the thermal conductivity coefficient of the fluid, respectively.

The local heat transfer coefficient was given by

$$h_x = -k \frac{\frac{\partial T}{\partial n}}{T_f - T_w}, \quad (7)$$

where T_w, T_f denote the wall temperature and the fluid temperature, respectively and $\partial T / \partial n$ denotes temperature gradient normal to the surface.

The average Nusselt number was obtained from equation

$$\text{Nu}_{\text{ave}} = \frac{1}{L_{\text{total}}} \int_0^{\text{total}} \text{Nu}(x) dx. \quad (8)$$

To calculate the friction factor, the following equation is used:

$$f = \frac{\Delta p H}{2\rho LV^2}, \quad (9)$$

where Δp is the pressure drop across the microchannel.

For general evaluation of thermal and flow performance for microchannels, the relations between Nusselt number for the microchannel with obstacles and the smooth microchannel $\frac{Nu_o}{Nu_s}$ and the relations between friction factor for the microchannel with obstacles and the smooth microchannel $\frac{f_o}{f_s}$ are adopted. These relations are used in the definition of the thermal enhancement factor, which is presented as:

$$\eta = \frac{\frac{Nu_o}{Nu_s}}{\left(\frac{f_o}{f_s}\right)^{1/3}}, \quad (10)$$

where f_o , Nu_o denote friction factor and Nusselt number for the microchannel with obstacles, f_s , Nu_s denote friction factor and Nusselt number for the microchannel without obstacles (smooth microchannel).

Steady-state forced convection in a microchannel was studied. A constant fluid temperature at the inlet was 20°C. A constant wall temperature of 60°C was assumed.

Numerical simulations were performed for three different values of obstacle height and four Reynolds numbers: 20, 50, 100, 200. To obtain hydrodynamics and heat characteristics in the structured microchannels, the equations (1–(4)) were solved by the CFD method. Simulations were performed using the CFD solver of ADINA R&D, Inc. 9.8.0 [25]. FEM (Finite Element Method) was used for the simulations. To simulate the fluid flow in the domain, we used the laminar model, in which the standard pressure interpolation schematic was applied. To solve the pressure-velocity coupling problem, the SIMPLE method was applied.

The validation of numerical data was obtained by comparing with the experimental values from [21].

The analyses of microchannels with thin obstacles and smooth microchannels were based on a structured mesh. The 2D quadrilateral elements were used for the grid. The meshes consisted of between maximum 20800 elements and 21361 nodes, and minimum 20200 elements, and 20881 nodes. Additionally, prior to the analysis, a grid sensitivity analysis was performed. The Grid Convergence Index [26] can be computed as

$$GCI = \frac{f_s}{R^c - 1} \left| \frac{v_{H2} - v_{H1}}{u_{H1}} \right| \cdot 100, \quad (11)$$

where f_s – the safety factor, $f_s = 1.25$ [18], R – the density factor, c – the order of convergence ($c = 2$), v_{H1} , v_{H2} – the chosen parameters (for the calculations max velocity in the x plane was accepted), H_1 , H_2 – the number of finite elements for two types of grid, respectively.

For a grid, where the finite element length was $5 \mu\text{m}$, CGI below 0.1% was obtained.

3. Results and discussion

Two-dimensional models of microchannels with thin obstacles on the walls were looked into using a the CFD solver ADINA. The following 20 cases of microchannels with thin obstacles were explored to analyze the effect of the obstacle height, various inlet velocity on flow, and thermal characteristics.

Simulations were executed for parameters with various values presented in Table 1. The development of heat transfer and water vortices in the microchannel was the target of observation for three types of water flow defined by the Re values of 20, 50 and 200 using non-dimensional parameters h/H .

Table 1. The dimensions of obstacle

H [μm]	h/H	w [μm]	w/h
100	0.25	50	0.5
200	0.5	50	0.25
300	0.75	50	0.17

3.1. Effect of an aspect ratio of the obstacle height (h/H) on the field of flow

The distribution of water flow in the microchannel characterized by thin obstacles was analyzed to demonstrate how the fluid field is influenced by their height. The obstacles of rectangular shape of width equal to $w = 10 \mu\text{m}$ and height aspect ratio $h/H = 0.25$, $h/H = 0.5$, $h/H = 0.75$ were the object of investigation. Fig. 2 depicts structures of flow in the microchannel with thin obstacles. Here, the streamlines are presented for $Re = 50$. It is noticed that the existence of obstacles that influence the flow makes the distribution of velocity of the flow structure different from the flow in smooth channel (Fig. 2d). Figs. 2 a, b, c illustrate the influence of the height of rectangular obstacles placed alternately on the channel walls on the water flow after taking into account the hydrodynamic entry length. Differences in the contours of the streamlines for water flows occurring in the microchannel can be observed for the obstacles of the varying height aspect ratios of $h/H = 0.25$, $h/H = 0.5$, $h/H = 0.75$. A recirculation zone appears behind the

obstacles. The measure of vorticity is a circulation. Notwithstanding, the vortex may be characterized by the recirculation zone's length. The method we follow in this paper is the one which was used to define the vortex on the obstacle's back, i.e., downstream from the obstacle. The recirculation zone's length was determined as the distance between the obstacle and the vortex's closure. As foreseen, it can be observed without any doubt, that the recirculation zone elongates with the increase in the value of the aspect ratio of obstacle's height. The results show that the length of recirculation zone increases with the obstacle height.

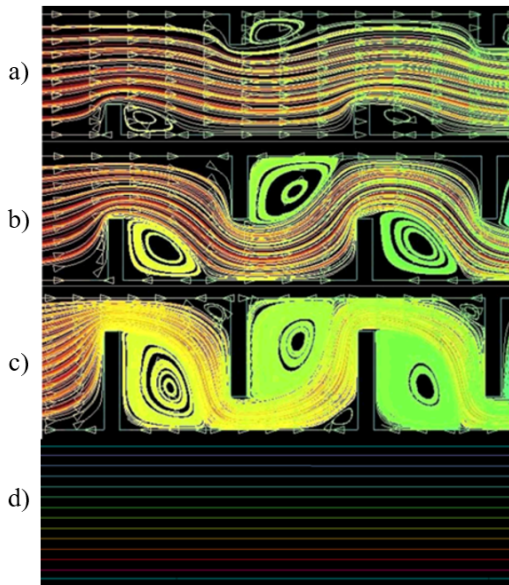


Fig. 2. Streamlines distribution in three microchannels with rectangular obstacles on the walls, varying in the height of the obstacles: a) $h/H = 0.25$, b) $h/H = 0.5$, c) $h/H = 0.75$; in each flow $Re = 50$, $s = 1H$, d) smooth channel

In Fig. 3, we have plotted the velocity distribution for $Re = 50$. The maximum velocity in the smooth microchannel always occurs near the center of the microchannel. The maximum velocity for the microchannel with obstacles is positioned towards the sidewall where there is no obstacle. Fig. 3 shows that the velocity is very low in the recirculation zone. Low velocity in the recirculation zone can reduce the heat transfer. The difference in velocity in the x -direction in the microchannel for the aspect ratio of obstacle's height $h/H = 0.25$ is smaller than in the other microchannels. It is noted that the flow direction changes periodically due to the periodic obstruction of the obstacles. The velocity difference in the x -direction in the microchannel increases with the increase of the obstacle's height.

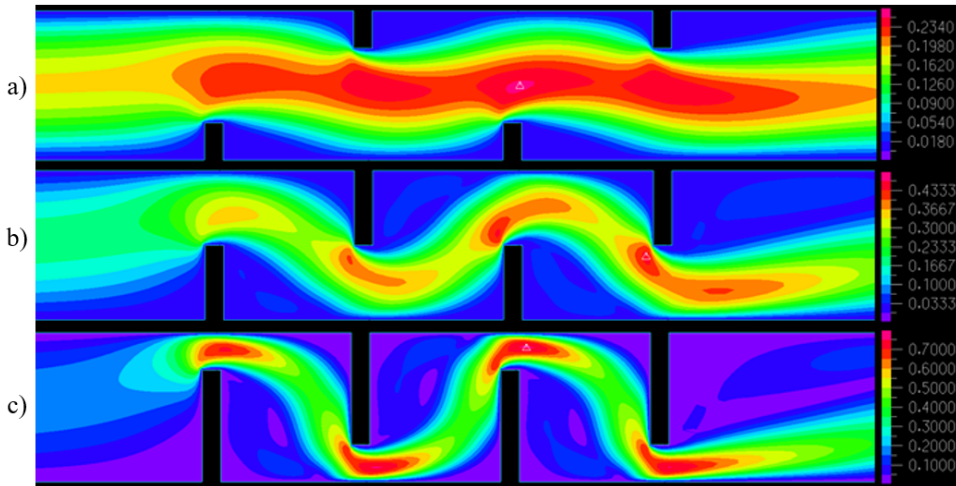


Fig. 3. Water velocity distributions V [m/s] in three microchannels with rectangular obstacles on the walls, varying in the height of the obstacles: a) $h/H = 0.25$, b) $h/H = 0.5$, c) $h/H = 0.75$; in each flow $Re = 50$, $s = 1H$

3.2. Effect of an aspect ratio of obstacle height (h/H) on pressure drop

Fig. 4 introduces the pressure drop along the length of microchannel at $Re = 50$. As shown in the figure, the pressure drop is higher for the microchannel with obstacles than for a smooth channel (without obstacles) along the channel length. This is due to the combined effects of flow disruption and the development of the recirculation zone past the obstacles, as shown in Fig. 2. A high pressure drop in the microchannel causes a large pumping power in the channel. The results demonstrate that the effect of the aspect ratio of obstacle's height $h/H = 0.25$ on the flow field's disturbance is much less evident than in the instance of the height aspect ratio of obstacle $h/H = 0.5$ and $h/H = 0.75$, but is greater than for the smooth microchannel.

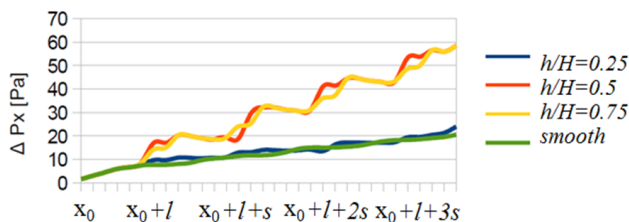


Fig. 4. Pressure drop along the local section in the microchannel, in each flow $Re = 50$

3.3. Effect of the Reynolds number on the velocity field

In Fig. 5, the vectors of water velocity in the microchannel are depicted in dependence on the values of Reynolds number, range of which is from 20 to 200. The obstacles with the aspect ratio of its height $h/H = 0.25$ were accounted for. The conclusion is that the recirculation zone's length raises with the increase of the Reynolds number.

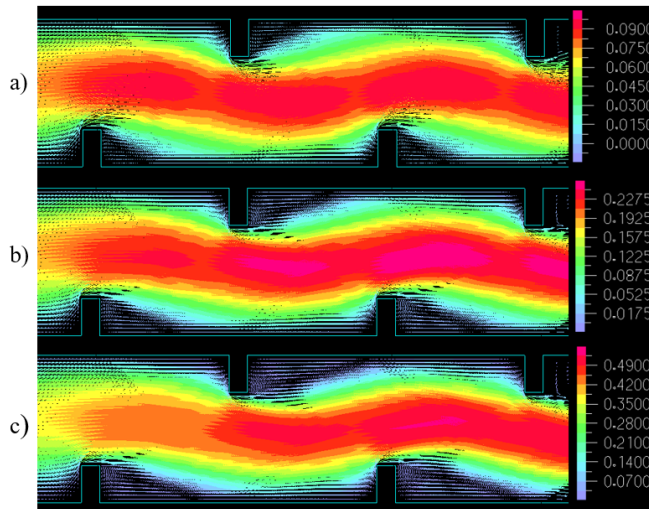


Fig. 5. Water velocity distributions V [m/s] in three microchannels with rectangular obstacles on the walls, varying in the Reynolds number: a) $Re = 20$, b) $Re = 50$, c) $Re = 100$; in each flow, $h/H = 0.25$, $s = 1H$

3.4. Characteristics of heat transfer

The objects of comparison were the distributions of heat transfer in the microchannel with thin obstacles, which made it possible to visualize the influence of their height on the temperature field. Fig. 6 depicts the representation of the field of temperature in the microchannel for $Re = 50$. These were achieved for different values of aspect ratios of the obstacle's heights. Diverse fields of temperature for flows where aspect ratio of the obstacle's height is $h/H = 0.25$, $h/H = 0.5$, $h/H = 0.75$ are noticed. The distribution zone of temperature behind the obstacles is analogous to the distribution of the fluid flow shown in Fig. 3. The results demonstrate that the distribution of temperature is dependent on the height of obstacle. Moreover, it can likewise be found that it is analogous to the zone of recirculation downstream of the obstacles, as demonstrated in Fig. 2.

Fig. 7 shows the local Nusselt numbers along the length of the microchannel L at $Re = 50$. Variations of local Nusselt numbers for rectangular obstacles are displayed for three distinct values of aspect ratio of obstacle's height and a smooth

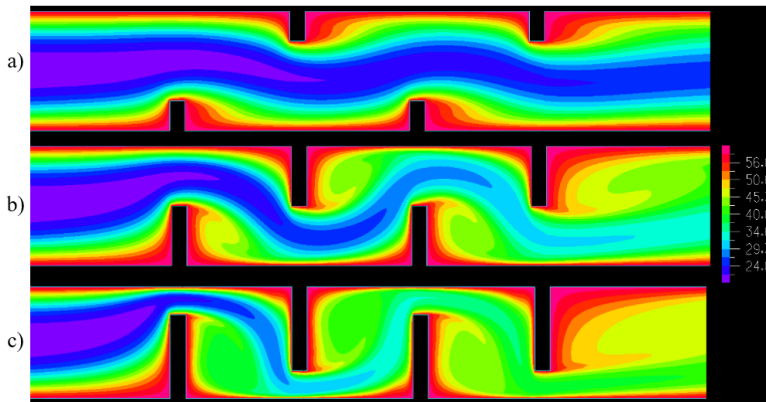


Fig. 6. Water temperature distribution T [°C] in three microchannels with rectangular obstacles on the walls, varying in the height of the obstacles: a) $h/H = 0.25$, b) $h/H = 0.5$, c) $h/H = 0.75$; in each flow $Re = 50$, $s = 1H$

channel. The cases of flow in microchannels with obstacles show that for the aspect ratio of height $h/H = 0.25$, $h/H = 0.5$, $h/H = 0.75$ the local Nusselt number decreases past the obstacles, and then increases. The results show that the local distribution of Nusselt numbers depends on the height of the obstacle. Also, it can be found that the decrease in the local Nusselt numbers corresponds to the recirculation zones downstream of the obstacles, as shown in Fig. 2. The results reveal greater values of local Nusselt numbers in the case of the microchannels including obstacles in relation to the channel which is smooth.

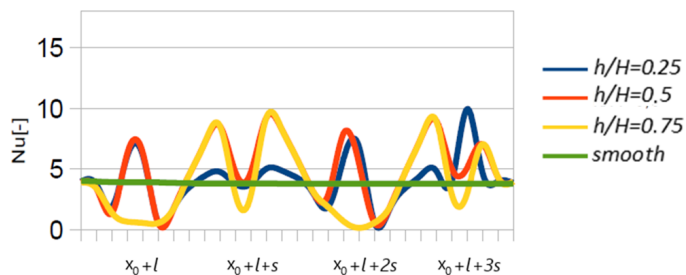


Fig. 7. Local Nusselt number along the local section in the microchannel, in each flow $Re = 50$

To further evaluate the heat transfer performance and the pressure variation in the microchannel with obstacles and to compare them with the smooth microchannel the results are presented in Fig. 8.

As can be seen in Fig. 8, the emplacement of obstacles on the walls of the microchannel with the aspect ratio of obstacles' height $h/H = 0.25$, $h/H = 0.5$, $h/H = 0.75$ yields the relations between Nusselt number for the microchannel with obstacles and the smooth microchannel $\frac{Nu_o}{Nu_s}$ of 1.93, 1.98, 1.2, respectively, and

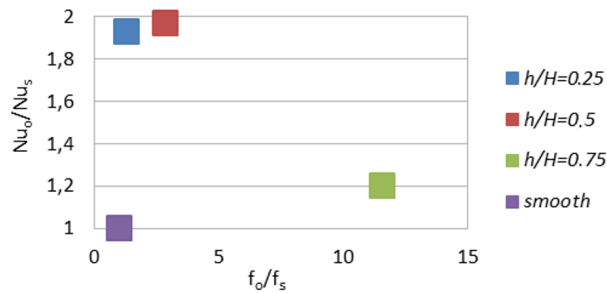


Fig. 8. The relations between Nusselt number for the microchannel with obstacles and smooth microchannel Nu_o/Nu_s and the relations between the friction factor for the microchannel with obstacles and smooth microchannel f_o/f_s for microchannels with rectangular obstacles on the walls and smooth microchannel, in each flow $Re = 50$

the relations between the friction factor for the microchannel with obstacles and the smooth microchannel $\frac{f_o}{f_s}$ of 1.31, 2.86, 11.58, respectively. In the case of the thermal enhancement factor, it is noticeable that the thermal enhancement factor η increases as the aspect ratio of height increases from $h/H = 0.25$ to $h/H = 0.5$, and then decreases for the height aspect ratio $h/H = 0.75$ to the value slightly above the one for the smooth microchannel.

4. Conclusions

The main goal of this work was the modeling of the heat transfer processes and fluid flow occurring in microchannels with thin obstacles placed on the side of the channel and the numerical analysis thereof. The results of analysis proved a considerable influence of emplacement of several obstacles in the channel as well as their height on the mass and heat exchange. The main mechanism influencing the heat transfer was found to be the formation of recirculation zones behind obstacles. This also causes a significant increase in the pressure. In accordance with the results, the magnitude of recirculation zones grows with the height of obstacles. Similarly, increasing the value of Re leads to enlargement of the averaged and local heat transfer in the channels. On the basis of on the results, it can be concluded that:

- The main mechanism of influence on fluid flow and heat transfer is the creation of recirculation zones behind thin obstacles.
- The height of the thin obstacles influences the length of the recirculation zone past the obstacles in the microchannel. The length of these zones is increased as the height of the obstacles grows.
- The growth of Reynolds number makes the recirculation zones behind the obstacle longer.

- The microchannels with thin obstacles and high aspect ratio (h/H) exhibit more efficient heat transfer but at the same time a larger pressure drop compared to smooth channels.
- For high obstacles ($h/H > 0.5$), there is a large heat transfer. However, this results in increased pressure losses.
- For the high obstacles ($h/H > 0.5$), the heat transfer coefficient is almost doubled compared to a smooth channel.

The results obtained for a various heights of four thin obstacles provide the basis for the design of microchannels with thin obstacles in the channel. They make it possible to select the optimum heights of thin obstacles depending on the velocity of flow and heat transfer performance.

References

- [1] Y.-T. Yang and S. Yang. Numerical study of turbulent flow in two-dimensional channel with surface mounted obstacle. *International Journal of Heat and Mass Transfer*, 37(18):2985–2991, 1994. doi: [10.1016/0017-9310\(94\)90352-2](https://doi.org/10.1016/0017-9310(94)90352-2).
- [2] K. Sivakumar, T. Sampath Kumar, S. Sivasankar, V. Ranjithkumar, and A. Ponshanmugakumar. Effect of rib arrangements on the flow pattern and heat transfer in internally ribbed rectangular divergent channels. *Materials Today: Proceedings*, 46(9):3379–3385, 2021. doi: [10.1016/j.matpr.2020.11.548](https://doi.org/10.1016/j.matpr.2020.11.548).
- [3] T.M. Liou, S.W. Chang, and S.P. Chan. Effect of rib orientation on thermal and fluid-flow features in a two-pass parallelogram channel with abrupt entrance. *International Journal of Heat and Mass Transfer*, 116:152–165, 2018. doi: [10.1016/j.ijheatmasstransfer.2017.08.094](https://doi.org/10.1016/j.ijheatmasstransfer.2017.08.094).
- [4] W. Yang, S. Xue, Y. He, and W. Li. Experimental study on the heat transfer characteristics of high blockage ribs channel. *Experimental Thermal and Fluid Science*, 83:248–259, 2017. doi: [10.1016/j.expthermflusci.2017.01.016](https://doi.org/10.1016/j.expthermflusci.2017.01.016).
- [5] F.B. Teixeira, M.V. Altnetter, G. Lorenzini, B.D. do A. Rodriguez, L.A.O. Rocha, L.A. Isoldi, and E.D. dos Santos. Geometrical evaluation of a channel with alternated mounted blocks under mixed convection laminar flows using constructal design. *Journal of Engineering Thermophysics*, 29(1): 92–113, 2020. doi: [10.1134/S1810232820010087](https://doi.org/10.1134/S1810232820010087).
- [6] A. Korichi and L. Oufer. Numerical heat transfer in a rectangular channel with mounted obstacles on upper and lower walls. *International Journal of Thermal Sciences*, 44(7):644–655, 2005. doi: [10.1016/j.ijthermalsci.2004.12.003](https://doi.org/10.1016/j.ijthermalsci.2004.12.003).
- [7] L.C. Demartini, H.A. Vielmo, and S.V. Möller. Numeric and experimental analysis of the turbulent flow through a channel with baffle plates. *Journal of the Brazilian Society of Mechanical Sciences and Engineering*, 26(2):153–159, 2004. doi: [10.1590/S1678-58782004000200006](https://doi.org/10.1590/S1678-58782004000200006).
- [8] Y.T. Yang and C.Z. Hwang. Calculation of turbulent flow and heat transfer in a porous-baffled channel. *International Journal of Heat and Mass Transfer*, 46(5):771–780, 2003. doi: [10.1016/S0017-9310\(02\)00360-5](https://doi.org/10.1016/S0017-9310(02)00360-5).
- [9] G. Wang, T. Chen, M. Tian, and G. Ding. Fluid and heat transfer characteristics of microchannel heat sink with truncated rib on sidewall. *International Journal of Heat and Mass Transfer*, 148:119142, 2020. doi: [10.1016/j.ijheatmasstransfer.2019.119142](https://doi.org/10.1016/j.ijheatmasstransfer.2019.119142).
- [10] S. Mahjoob and S. Kashkuli. Thermal transport analysis of injected flow through combined rib and metal foam in converging channels with application in electronics hotspot removal. *International Journal of Heat and Mass Transfer*, 177:121223, 2021. doi: [10.1016/j.ijheatmasstransfer.2021.121223](https://doi.org/10.1016/j.ijheatmasstransfer.2021.121223).

- [11] L. Chai, G.D. Xia, and H.S. Wang. Numerical study of laminar flow and heat transfer in microchannel heat sink with offset ribs on sidewalls. *Applied Thermal Engineering*, 92:32–41, 2016. doi: [10.1016/j.applthermaleng.2015.09.071](https://doi.org/10.1016/j.applthermaleng.2015.09.071).
- [12] Y. Yin, R. Guo, C. Zhu, T. Fu, and Y. Ma. Enhancement of gas-liquid mass transfer in microchannels by rectangular baffles. *Separation and Purification Technology*, 236:116306, 2020. doi: [10.1016/j.seppur.2019.116306](https://doi.org/10.1016/j.seppur.2019.116306).
- [13] A. Behnampour O.A. Akbari, M.R. Safaei, M. Ghavami, A. Marzban, G.A.S. Shabani, M. Zarringhalam, and R. Mashayekhi. Analysis of heat transfer and nanofluid fluid flow in microchannels with trapezoidal, rectangular and triangular shaped ribs. *Physica E: Low-Dimensional Systems and Nanostructures*, 91:15–31, 2017. doi: [10.1016/j.physe.2017.04.006](https://doi.org/10.1016/j.physe.2017.04.006).
- [14] M.R. Gholami, O.A. Akbari, A. Marzban, D. Toghraie, G.A.S. Shabani, and M. Zarringhalam. The effect of rib shape on the behavior of laminar flow of oil/MWCNT nanofluid in a rectangular microchannel. *Journal of Thermal Analysis and Calorimetry*, 134(3):1611–1628, 2018. doi: [10.1007/s10973-017-6902-3](https://doi.org/10.1007/s10973-017-6902-3).
- [15] O.A. Akbari, D. Toghraie, A. Karimipour, M.R. Safaei, M. Goodarzi, H. Alipour, and M. Dahari. Investigation of rib's height effect on heat transfer and flow parameters of laminar water-Al₂O₃ nanofluid in a rib-microchannel. *Applied Mathematics and Computation*, 290:135–153, 2016. doi: [10.1016/j.amc.2016.05.053](https://doi.org/10.1016/j.amc.2016.05.053).
- [16] B. Mondal, S. Pati, and P.K. Patowari. Analysis of mixing performances in microchannel with obstacles of different aspect ratios. *Journal of Process Mechanical Engineering*, 233(5):1045–1051, 2019. doi: [10.1177/0954408919826748](https://doi.org/10.1177/0954408919826748).
- [17] L. Chai, G.D. Xia, and H.S. Wang. Parametric study on thermal and hydraulic characteristics of laminar flow in microchannel heat sink with fan-shaped ribs on sidewalls – Part 2: Pressure drop. *International Journal of Heat and Mass Transfer*, 97:1081–1090, 2016. doi: [10.1016/j.ijheatmasstransfer.2016.02.076](https://doi.org/10.1016/j.ijheatmasstransfer.2016.02.076).
- [18] P. Pontes, I. Gonçalves, M. Andredaki, A. Georgoulas, A.L.N. Moreira, and A.S. Moita. Fluid flow and heat transfer in microchannel devices for cooling applications: Experimental and numerical approaches. *Applied Thermal Engineering*, 218:119358, 2023. doi: [10.1016/j.applthermaleng.2022.119358](https://doi.org/10.1016/j.applthermaleng.2022.119358).
- [19] B.K. Srihari, A. Kapoor, S. Krishnan, and S. Balasubramanian. Computational fluid dynamics studies on the flow of fluids through microchannel with intentional obstacles. *AIP Conference Proceedings*, 2516(1):170003. doi: [10.1063/5.0108550](https://doi.org/10.1063/5.0108550).
- [20] T. Grzebyk and A. Górecka-Drzazga. Vacuum microdevices. *Bulletin of the Polish Academy of Sciences: Technical Sciences*, 60(1):19–23, 2012. doi: [10.2478/v10175-012-0004-y](https://doi.org/10.2478/v10175-012-0004-y).
- [21] M. Kmiołek and A. Kucaba-Piętal. Influence of slim obstacle geometry on the flow and heat transfer in microchannels. *Bulletin of the Polish Academy of Sciences: Technical Sciences*, 66(2):111–118, 2018. doi: [10.24425/119064](https://doi.org/10.24425/119064).
- [22] S. Baheri Islami, B. Dastvareh, and R. Gharraei. An investigation on the hydrodynamic and heat transfer of nanofluid flow, with non-Newtonian base fluid, in micromixers. *International Journal of Heat and Mass Transfer*, 78:917–929, 2014. doi: [10.1016/j.ijheatmasstransfer.2014.07.022](https://doi.org/10.1016/j.ijheatmasstransfer.2014.07.022).
- [23] S. Baheri Islami, B. Dastvareh, and R. Gharraei. Numerical study of hydrodynamic and heat transfer of nanofluid flow in microchannels containing micromixer. *International Communications in Heat and Mass Transfer*, 43:146–154, 2013. doi: [10.1016/j.icheatmasstransfer.2013.01.002](https://doi.org/10.1016/j.icheatmasstransfer.2013.01.002).
- [24] C.K. Chung, C.Y. Wu, and T.R. Shih. Effect of baffle height and reynolds number on fluid mixing. *Microsystem Technologies*, 14(9–11):1317–1323, 2008. doi: [10.1007/s00542-007-0511-1](https://doi.org/10.1007/s00542-007-0511-1).
- [25] I. Adina R&D. *Theory and Modling Guide*, vol. III: ADINA CFD&FSI, Report ARD. 2019.
- [26] P.J. Roache. *Verification and Validation in Computational Science and Engineering*. Hermosa Publishers, 1998.